JOURNAL OF AIRCRAFT
Vol. 37, No. 4, July–August 2000

Convergent-Flow-Derived Waveriders

Yu. P. Goonko,* I. I. Mazhul,† and G. N. Markelov‡
Russian Academy of Sciences, 630090, Novosibirsk, Russia

Results are presented of a study on the aerodynamics of a new type of waverider derived from supersonic axisymmetric flows inside constricting ducts, specifically conical trumpet ducts. In such a duct, an initial shock wave arises from its leading edge, and the compression flow downstream of this shock has streamlines converging toward the flow axis. This flow is chosen as a basic flow for the waverider design. The simplest convergent-flow-derived waveriders are constructed with a lifting surface with a transverse-concave arc-shaped contour. They are compared with known types of waveriders constructed based on uniform flows behind plane oblique shock waves or divergent flows behind axisymmetric conical shock waves. The characteristics of convergent waveriders as lifting configurations are analyzed with the lift and drag coefficients, the lift-to-drag ratio, and the integral heat fluxes through the waverider surfaces determined. The possibilities of using these new waveriders as forebodies for hypersonic vehicles powered by airbreathing engines are also estimated. The flowfield characteristics near the lower lifting surface of the waverider as a precompression surface arranged upstream of the inlet are considered in this connection.

Nomenclature

C_D = drag coefficient, $D/(q_\infty S_{\rm pl})$
C_L = lift coefficient, $L/(q_\infty S_{\rm pl})$
L/D = lift-to-drag ratio
L_w = waverider length, m
$\bar{L}_w$ = relative length of a waverider, L_w/R_0
M = flow Mach number
$\bar{p}$ = relative static pressure, p/p_∞
q_∞ = freestream dynamic pressure, Pa
$\bar{R}_e$ = relative radius of transverse curvature of a lifting surface in the end cross section of a waverider, R_e/R_0
$\bar{R}_s$ = relative radius of a trumpet-shaped shock wave, R_s/R_0
R_0 = radius of a constricting duct in the initial cross section, m
$S_{\rm pl}$ = reference planform area of a waverider, m^2
$\bar{x}, \bar{r}$ = relative longitudinal and radial coordinates, x/R_0 and r/R_0, respectively
$\bar{x}_a$ = relative longitudinal coordinate of the waverider aerodynamic center, x_a/L_w
$\bar{x}_e$ = relative longitudinal coordinate of the waverider end cross section, x_e/R_0
δ_c = cone angle, deg
δ_d = angle of inclination of a conical duct wall to the duct axis, deg
δ_w = wedge angle, deg
θ = angle of inclination of a flow velocity vector to the duct axis, deg
τ = volumetric factor, $\sqrt[3]{(\Omega^2)}/S_{\rm pl}$
φ = half-angle of the arc contour sector, deg
Ω = waverider volume, m^3

Subscripts

s = shock wave
∞ = freestream values

Received 2 June 1999; revision received 14 March 2000; accepted for publication 3 April 2000. Copyright © 2000 by the American Institute of Aeronautics and Astronautics, Inc. All rights reserved.

*Head of Research Group, Experimental Aerodynamics Laboratory, Siberian Branch, Institute of Theoretical and Applied Mechanics.
†Senior Research Scientist, Experimental Aerodynamics Laboratory, Siberian Branch, Institute of Theoretical and Applied Mechanics.
‡Senior Research Scientist, Computational Aerodynamics Laboratory, Siberian Branch, Institute of Theoretical and Applied Mechanics.

Introduction

IN the design of high-speed flying vehicles, methods are often used in which the aerodynamic surfaces are constructed as stream surfaces of known inviscid supersonic flows forming downstream of the shock waves. General concepts of this kind of design are discussed, for example, in Refs. 1–5. This trend is commonly called inverse design, in contrast to direct design methods. According to Maikapar and Keldysh,[5] in Russia, it also called gasdynamic design because in many cases the flows used are typically described by nonlinear equations or closed solutions of gasdynamics. This approach includes the design of waveriders, which are three-dimensional lifting configurations with leading edges lying on the surface of a shock wave of known shape. Simple shocked-flow solutions determined exactly analytically or numerically are usually employed. The simplest waverider is the Nonweiler caret wing[6,7] designed based on a uniform flow behind a plane oblique shock wave generated by a wedge. Design of waveriders from flows behind conical shock waves over circular and elliptic cones is well-known.[3,8–10] Note that, despite a great variety of different types of waveriders, they are usually derived from external flows forming around the bodies. On the whole such basic flows are divergent, that is, their streamlines are divergent toward the freestream flow direction.

Combining various flow patterns carved in a simple basic flow and assembling these flow patterns or the regions of different original flows can be used for gasdynamic design. This allows one to obtain multipieced or multishocked combined-design flows and, also, to construct configurations that satisfy different requirements imposed on flying vehicles. Examples of constructing complex waverider-type lifting configurations with inlets and engine ducts are given in Refs. 11–15. Note that many scientists, too numerous to be mentioned, have contributed to the waverider design effort.

Some papers on gasdynamic design deal with the three-dimensional inlets, called convergent.[16–18] They were constructed using supersonic shocked flows with streamlines converging in space toward the freestream flow direction, that is, on the basis of convergent flows. The flow convergence applied to construct the external compression section of such an inlet ensures, in particular, a compact, close to circular, cross-sectional inlet throat and engine duct. The wetted area of the walls of such engine ducts is smaller as compared to engines constructed with two-dimensional (flat) or axisymmetric inlets having a centerbody and a slot-shaped throat. This can facilitate the thermal protection of the walls of high-speed airbreathing engines. Convergent inlets also provide a higher level of flow compression in comparison with flat inlets with equal final angles of inclination of the inlet ramps. The designing of convergent inlets was performed using both supersonic axisymmetric

compression flows and combinations of two-dimensional shocked flows. One of the simple types of convergent inlets is constructed using supersonic axisymmetric compression flows inside constricting ducts[17,18] whose internal surfaces are conical or with other surfaces of revolution with a curved generatrix. Such an inlet has a nonswept leading edge; its ramp is constructed with a concave external compression surface having an arc-shaped transverse contour. From its characteristic shape, such an inlet can be called a shovel type.

A purpose of the waveriders, or their application, is one of the main factors specifying a type of flow chosen as the basic one for the waverider design. In the present paper, we consider waveriders that will ensure elevated levels of flow compression near the lifting surface in comparison with known waveriders derived from two-dimensional or conic flows. Following Ref. 19, they are constructed with the use of supersonic axisymmetric flows inside constricting ducts, trumpets, as just described for the convergent inlets derived from the same flows. In such a trumpet duct, an initial shock wave arises from its leading edge. The shock wave is also trumpet shaped, its generatrix in a meridian plane is curved, and the compression flow downstream of the shock has streamlines converging toward the duct axis. Thus, the basic internal compression flows chosen for designing these waveriders are convergent, as compared to two-dimensional and axisymmetric supersonic external divergent flows used for designing known waveriders. From the main feature, convergence of the original basic flows, the waveriders constructed with the use of these former flows will be called convergent-flow derived or simply convergent.

The waveriders so obtained can be considered as a basis for designing more general lifting configurations of hypersonic vehicles. In addition, these waveriders can be used as forebodies of vehicles powered by airbreathing engines. They have a transverse-concave external lifting-compressing surface, under which it is convenient to arrange the mentioned convergent shovel-type inlets. We analyze the characteristics of the waveriders from the viewpoint of both of these applications. Results of the analysis of lift force, lift-to-drag ratio, and integral heat fluxes to the surfaces of these waveriders are presented, that is, the waveriders are considered as lifting configurations. The parameters of the flowfield near the lower lifting surface of the convergent waveriders, interpreted as a precompression surface upstream of the inlet, are analyzed. The average parameters of the airstream adjacent to the lifting–compressing surface and captured by the inlet are determined.

Note that in the past few decades various numerical techniques for the solution of flowfields around waveriders have been used, including Euler solvers and Navier–Stokes simulation. They are powerful means for studying off-design flow regimes of waveriders and for including optimization techniques. However, the main objective of setting up the presented problem was to put forward new waveriders both as lifting configurations and precompression forebodies. It is an initial step in designing these waveriders and subsequently studying them in more detail. From this standpoint, simple methods are very appropriate to design their shape, preliminary to estimating aerodynamic characteristics, to analyze their performance, and to present the main properties. Such are, indeed, the methods applied to our problem and specified hereinafter. In addition, convergent waveriders are compared with known types of waveriders of a caret wing type derived from uniform flows behind plane oblique shock waves and those constructed on the basis of divergent flows behind axisymmetric conical shock waves. Such a comparison enables a more comprehensible presentation of the convergent waveriders.

Note also that many special problems on waverider optimization with different criteria and limitations could be set up. Such problems are rather arduous, especially with using numerical methods. That is why the authors do not as yet setup any optimization problems. Nevertheless, one can see some optimal parameters of the waverider under consideration from the parametric relationships to be presented.

Design of Convergent Waveriders

The principle of designing a convergent waverider from an axisymmetric internal flow inside a constricting conical duct trumpet

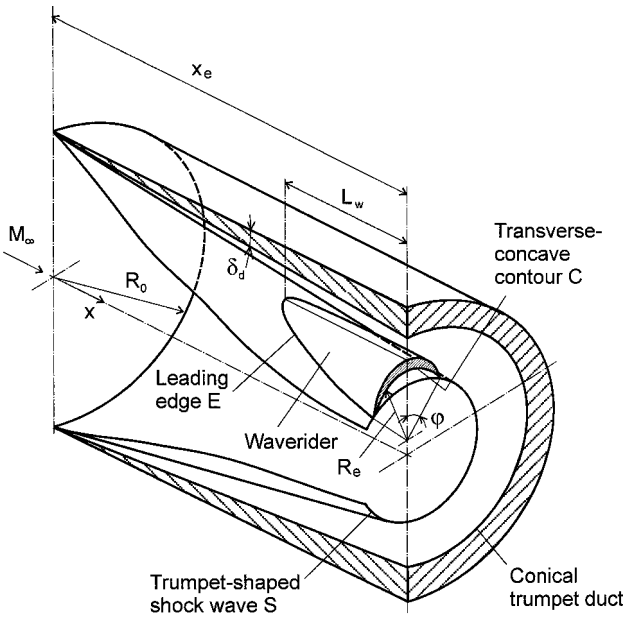

Fig. 1 Designing convergent waveriders on the basis of the axisymmetric flow inside a constricting conical duct.

is shown in Fig. 1. A uniform freestream flow with a Mach number M_∞ enters the trumpet duct. The duct geometry is defined by the radius R_0 of the initial cross section at $x = 0$ and the angle δ_d of the duct wall inclination to the duct axis. Downstream of the initial cross section, an axisymmetric flow with a trumpet-shaped shock wave S forms. Note that the basic flow is convergent, that is, its streamlines converge to the duct axis that is also the flow axis, and this flow is independent of the initial radius R_0 in coordinates normalized to R_0. Furthermore, some general features of the initial shock wave that follow from the flow axisymmetry should be noted. This shock is weak, and the local supersonic flow immediately behind it is two dimensional at the leading edge. The slope of the shock wave increases progressively downstream, becomes strong, and transforms to a normal shock at the flow axis. Thus, the resultant flow forming behind the initial shock wave includes regions of both supersonic and subsonic flow. Leaving aside a question as to the conditions for which such flows occur, note that only the region of supersonic flow is used for waverider design.

We consider convergent waveriders with a smooth transverse-concave lower lifting surface of a simple arc-shaped transverse contour. The latter was chosen by reasoning that the said lower surface shape of the waverider as a precompression forebody fits in with the arc-shaped leading edge of a convergent shovel-type inlet arranged downstream. For convergent waveriders as lifting bodies, this contour can be considered as a generic example to demonstrate their characteristics. Note that any other cross-sectional contours (power law functions, hyperellipse, etc.) could be used, as necessary. The arc contour C of radius R_e is prescribed in a certain cross section x_e, which is used as the end cross section for waverider design. The radius R_e determines the transverse curvature of the lifting surface as a whole. The half-angle φ of the arc sector of the contour C is also used for defining the waverider geometry. The contour C is located between the shock wave and the duct wall. It does not intersect the duct circle contour, but can be tangent to the latter. Because of the geometry of the flow region in the considered cross section, the curvature of the contour C is always greater than the curvature of the shock wave S. The position of the center of the circle of contour C along the vertical axis is uniquely determined by the parameters R_e and φ, considering that the ends of the arc C lie on the shock wave circle in the said cross section.

The construction of the lifting surface begins from the end cross section with streamlines of the basic flow passing through the contour C and reconstructed upstream. The leading edge of the waverider is formed by the line E of intersection of the lifting surface

and the shock wave S. The upper nonlifting surface of the waverider is constructed as a cylindrical surface with generatrices parallel to the freestream direction.

Calculations of the basic inviscid, supersonic, axisymmetric flow for the convergent waverider design were performed with the use of the well-known method of characteristics. The method goes back to Refs. 20 and 21; its effective implicit finite difference scheme was developed in Refs. 22 and 23. The major features of these procedures were also presented in Ref. 24. The characteristic network is constructed concurrently with the shock wave emanating from the leading edge of the duct. The network construction is reduced to the iterative solution of a few elementary tasks on determination of the mesh points on the shock wave, on the body surface, on the axis, and in the flowfield. For a point on the body surface, the boundary condition requires the normal velocity component to be zero. A point on the shock wave is calculated, as usually in the method of characteristics, from the relations for one of the characteristics and the Rankine–Hugoniot relations that must be satisfied on the shock wave properly. The flow parameters are calculated along the characteristics, but the calculation results are interpolated to matrices of the flow parameters determined in cross sections specified along the longitudinal axis. The size of computational cells along the characteristics is chosen so that the number of cross sections in which the matrices are determined varied within $N_x = 100$–200 depending on the size of the flow region used for the design. The calculation accuracy is controlled according to recommendations in Ref. 23 based on the use of the streamfunction. The difference between the two stream function values obtained in a calculation point on the duct wall is estimated. One value was obtained by integration along the characteristic of the first family; the other corresponded to the value calculated along the surface streamline emanating from the leading edge of the trumpet duct. The difference did not exceed 0.01%.

The stream function was also used to determine the streamlines and, hence, to design the lifting surface of the convergent waverider. For this purpose, a set of $N_p = 50$–100 points was prescribed on the transverse contour C defined in the end cross section with the coordinate x_e. The points were distributed uniformly along the contour. A certain value of the stream function calculated from the basic axisymmetric flowfield data corresponds to each point of the set. Based on this value, the respective streamline is reconstructed upstream to its intersection with the trumpet-shaped shock wave. The set of resultant streamlines determines the lower lifting surface, and the points of intersection of these streamlines with the initial trumpet-shaped shock wave determine the leading edge E of the waverider. The error in the construction of the lifting surface and the leading edge was determined and was dependent on the number of points N_p used in dividing the transverse contour. It was estimated integrally by the changes in the lift coefficient of the waverider and the flow rate of the airstream that can be captured by an inlet arranged under the lifting surface downstream of the end cross section. The inlet-captured airstream is assumed to be bounded by the waverider surface and the shock wave in the end cross section. The flow rate is first calculated from the parameters of the freestream tube bounded by the leading edges of the waverider and the shock wave contour in the end cross section. It is also determined from integration of parameters of the flow under the lifting surface in the end cross section. The construction algorithm that was used ensured an error of less than 0.1% for both integral characteristics estimated already for $N_p = 50$.

Continuing with the waverider definition, we outline the pertinent parameters. The given Mach number M_∞, the radius R_0 of the conical trumpet duct in the initial cross section, and the angle δ_d of the duct wall inclination determine the basic flowfield. The waverider geometry proper is determined by three independent parameters. The relative radius of the lower lifting surface $\bar{R}_e$ and the half-angle φ of the sector of the arc of the contour C in the end cross section (see Fig. 1) are prescribed. Furthermore, note that there is a longitudinal pressure gradient in the basic flowfield in the downstream direction along the duct wall or along a streamline. Therefore, the geometric and aerodynamic characteristics of a waverider under consideration should also depend on its longitudinal position in the basic flowfield. This position can be characterized by the relative longitudinal coordinate $\bar{x}_e$ of the end cross section of the waverider that completes the definition of geometrical parameters. The length L_w of a waverider constructed is evident from the intersection of the streamline passing the contour C and the shock wave line emanating from the leading edge of the duct in the plane of symmetry.

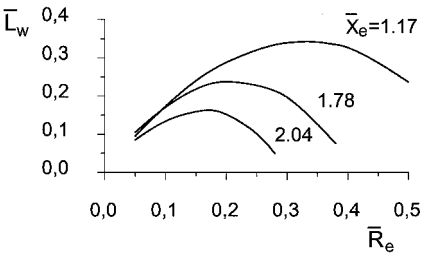

Fig. 2 Relative length of convergent waveriders: $M_\infty = 6$, $\delta_d = 10$ deg, and $\varphi = 45$ deg.

The length of the convergent waverider is exemplified in Fig. 2 for the freestream Mach number $M_\infty = 6$, the inclination angle of the trumpet duct wall $\delta_d = 10$ deg, and the sector half-angle of the arc contour $\varphi = 45$ deg. In Fig. 2, the relative length $\bar{L}_w$ is plotted as a function of the relative radius $\bar{R}_e$ characterizing the transverse curvature of the lifting surface of the waveriders for several values of the longitudinal coordinate $\bar{x}_e$. Obviously, for $R_e = 0$ or R_s, we have $L_w = 0$; hence, the relative length $\bar{L}_w$ of the waveriders has a maximum depending on $\bar{R}_e$. At the given $\bar{R}_e$, the farther downstream the waverider is located, that is, the greater the coordinate $\bar{x}_e$, the smaller is the waverider length owing to the bending of the trumpet-shaped shock wave to the flow axis and the increase in its slope.

The convergent waveriders constructed from the parameters just mentioned, that is, the free-stream Mach number $M_\infty = 6$, the inclination angle of the trumpet duct wall $\delta_d = 10$ deg, and the sector half-angle of the arc contour $\varphi = 45$ deg, will be considered as a generic example to demonstrate their characteristics. When necessary for comparison, we will also present the characteristics of the simplest waverider, which is the Nonweiler caret wing[7] derived from a uniform flow behind a plane shock wave, and a cone-derived waverider. The latter were constructed for the same freestream Mach number M_∞ and wedge angle $\delta_w = \delta_d$ or cone angle $\delta_c = \delta_d$.

Some Properties of the Flows Basic for Convergent Waverider Designing

Let us first consider some properties of supersonic inviscid flows inside constricting conical trumpet ducts, among which the basic flow is chosen for designing the waveriders under study. As already noted, these flows were calculated by the method of characteristics.[23]

The flow pattern in a longitudinal axial section is presented in Fig. 3 (for $M_\infty = 6$ and $\delta_d = 10$ deg). The flow in a trumpet duct begins from a locally two-dimensional flow behind an oblique shock wave at the leading edge. As the coordinate $\bar{x}$ increases, significant flow compression and an increase in the shock wave slope θ_s occur due to the convergence of the streamlines in reference to the flow axis. A curved shock wave emanating from the leading edge and a set of streamlines are shown in Fig. 3. The wall pressure increases downstream and becomes substantially greater than in the case of a uniform flow over a plane wedge with the same angle of wall inclination. The variations of the shock parameters and the flow pressure at the duct wall and immediately behind the shock vs the coordinate $\bar{x}$ are also plotted in Fig. 3. A high level of flow compression is a favorable factor from the viewpoint of both the aforementioned applications of the waveriders designed.

Note that within the range $\bar{x} = 0$–1.8, the nonuniformity of the flowfield across the duct is not too large. This is evident by a comparison of static pressure distributions along the duct wall and behind the shock wave (Fig. 3). Figure 4 shows the plots of the flow parameters as functions of the radial coordinate $\bar{r}$ for a few values $\bar{x} = \text{const}$. The pressure variation between the shock wave surface and the duct wall does not exceed ~2–3% for $\bar{x} \le 1.8$ and increases to ~8.6%

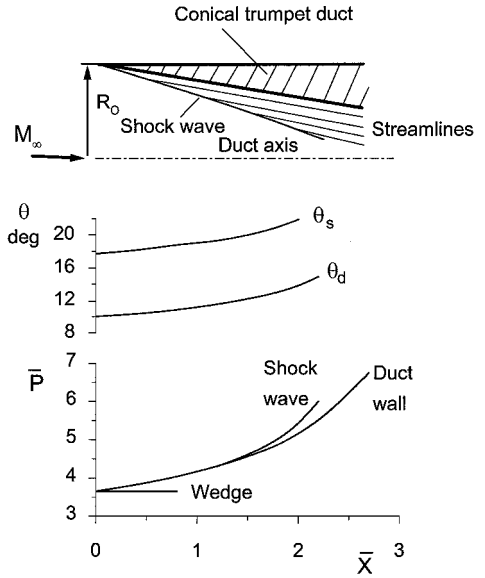

Fig. 3 Variation of parameters of the trumpet-shaped shock wave and the relative pressure immediately behind the shock wave and at the duct wall vs the coordinate $\bar{x}$: $M_\infty = 6$ and $\delta_d = 10$ deg.

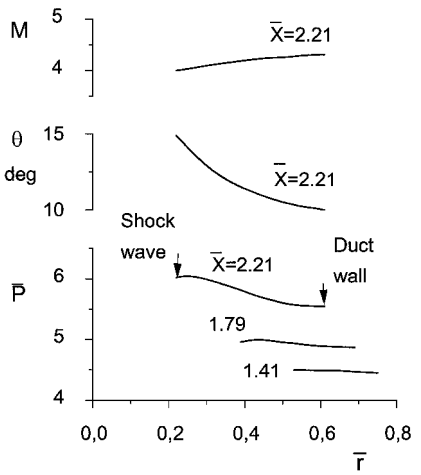

Fig. 4 Variation of the relative pressure, angle of inclination of the velocity vector, and local Mach number between the trumpet-shaped shock wave and the duct wall: $M_\infty = 6$ and $\delta_d = 10$ deg.

for $\bar{x} = 2.21$. Interestingly, there is a maximum in the dependence $\bar{p} = f(\bar{r})$, which is located near the shock wave. The pressure maximum shifts toward the shock wave as the longitudinal coordinate $\bar{x}$ increases, as noted in Ref. 24 for high values $M_\infty = 10.4$.

The value of the local-flow Mach number in a cross section $\bar{x} = \text{const}$ increases somewhat in a direction from the shock wave toward the duct wall (Fig. 4). For the considered example with $M_\infty = 6$ and $\delta_d = 10$ deg, however, the nonuniformity of the Mach number field is ~3.6 and ~7.3% for $\bar{x} = 1.79$ and 2.21, respectively. The angle of deflection, θ, of the velocity vector from the duct axis changes in the cross section $\bar{x} = \text{const}$ more significantly, decreasing to the duct wall (see Fig. 4). The value of this angle θ_d immediately behind the shock wave vs the longitudinal coordinate $\bar{x}$ is shown in Fig. 3. The angle θ_d increases downstream, due to an increase in the shock wave slope θ_s. As applied to waveriders, the angle θ_d will determine the slope of the lifting surface at their leading edge in the plane of symmetry $z = 0$.

An analysis of the properties of the basic internal flows shows that these flows can be used to construct convergent waveriders that ensure a high compression and rather uniform flowfield in a certain end cross section, where it is assumed an airbreathing engine inlet will be located. This is appropriate when the flow region chosen for waverider design lies within the range of values $\bar{x}$ at which the shock wave slope is not very large. At a further extension of this range downstream, however, the flow nonuniformity increases, particularly near the shock wave. In this aspect, the use of flow regions that correspond to large values of $\bar{x}$ possibly will not allow one to construct waveriders with a fairly uniform flowfield. At the same time, these regions can be effectively used to design waveriders with high required lift coefficients C_L. Notice that the contour C used for construction of these waveriders usually restricts only a part of the flow region between the shock wave and the duct wall. Therefore, the said nonuniformity of the flowfield under the lifting surface of the waverider proper can be significantly lower in this case in comparison with that mentioned earlier for the basic flow as a whole.

Let us exemplify the flow-field characteristics for a waverider with $\bar{x}_e = 1.78$ and $\bar{R}_e = 0.2$. The value $\bar{R}_e = 0.2$ defines the maximum length of the waverider for the determining parameters mentioned earlier. The level of relative static pressure on the waverider surface $\bar{p} = 4.7$–4.9 noticeably exceeds the value $\bar{p} = 3.67$ corresponding to the value behind a plane shock wave on a wedge with an angle $\delta_w = \delta_d$. The pressure increases by ~7% along the waverider length in the plane of symmetry. In the end cross section, the pressure on the lifting surface depends weakly on the span coordinate and also varies weakly between the lifting surface and the shock wave in the plane of symmetry. In both the latter cases, the nonuniformity of the pressure field does not exceed 3% and that of the Mach number field is less than ~0.5%. The nonuniformity of the total pressure distribution was estimated from the change in the pressure recovery factor $\sigma = p_0 / p_{0,\infty}$ in the case under discussion. Its magnitude is $\sigma = 0.65$–0.7, and the nonuniformity of the total pressure distribution is ~9% over the waverider span and ~3% between the lifting surface and the shock wave in the plane of symmetry. This means that the nonuniformity of flowfields obtained in the end cross section between the lifting surface and the shock wave of the convergent waverider is fairly small. The considered flow nonuniformity should be evaluated if the convergent waveriders are considered as precompression forebodies under which some inlets, specifically shovel-type convergent inlets, are arranged. It can be noted in this relation that this nonuniformity is small in comparison with that of flows through the convergent inlets proper (as presented in Ref. 18) or, for example that of a flow through the three-dimensional inlet with side compression wedges developed at NASA Langley Research Center.

Characteristics of Convergent Waveriders

The characteristics of the lift and drag forces and the lift-to-drag ratio were determined while considering the waveriders as lifting configurations. These characteristics correspond to design flow regimes, that is, to the flow parameters prescribed in the waverider design. The distribution of pressure forces is determined from the known inviscid flowfield, which is basic for designing.

From the viewpoint of obtaining real estimates of aerodynamic characteristics of the waveriders, it is necessary to include the friction forces in drag calculations. This is connected with the fact that aerodynamic configurations with transverse-concave lifting surfaces have a considerable wetted surface area S_w relative to their planform area S_{pl}, that is, the value of $\bar{S}_w = S_w / S_{\text{pl}}$, as it occurs, for example, for caret wings compared with delta wings. Correspondingly, the contribution of friction drag to the total drag and its effect on the total aerodynamic characteristics of concave configurations increases. Note that the relative wetted surface $\bar{S}_w$ of the convergent waveriders exemplified is almost independent of $\bar{x}_e$ and, within the examined range of $\bar{R}_e = 0.05$–0.5, amounts to $\bar{S}_w = 2.45$–2.2. The friction drag contribution varies directly with this value.

The flight of vehicles at high hypersonic speeds is accompanied by intense aerodynamic heating. Therefore, the overall level of heat to be absorbed by the cooling system to ensure allowable wall temperatures can be one of the factors that determines the possibility of employing convergent waveriders for such vehicles. In this connection, we also estimated the total heat flux Q to be removed by the cooling system to ensure a given temperature of the body wall $T_w = \text{const}$. The heat flux passing through the surfaces into the waverider body is determined by the difference between the convective q_w and the emitted radiative q_r heat fluxes. The input heat fluxes

were integrated along the streamlines on the wetted surfaces of the waverider. The integral input heat flux Q was normalized to the enthalpy of the freestream of a unit cross-sectional area $F_\infty = 1$ as

$$\bar{Q} = \frac{Q}{\Delta H_\infty}, \qquad Q = \int_0^{S_w} (q_w - q_r)\, \mathrm{d}S$$

$$\Delta H_\infty = \rho_\infty V_\infty F_\infty \int_{T_\infty}^{T_0} c_p(T)\, \mathrm{d}T$$

where $C_p(T)$ is the heat capacity of the air; V_∞, ρ_∞, T_∞, and T_0 are, respectively, the velocity, the density, and the static and total temperatures of the freestream. The quantity ΔH_∞ characterizes the maximal amount of energy of the freestream with the parameters M_∞ and T_∞, which can be transformed to aerodynamic heating of a vehicle after adiabatic deceleration of the freestream to stagnation parameters $M_\infty = 0$ and T_0.

The boundary layer on a surface (lower, or respectively upper) of the waverider was assumed to be fully turbulent and locally two dimensional along the streamlines. For its calculation, we used the method developed in Ref. 25 as applied to the turbulent boundary layer of a nonthermoinsulated flat plate. The method presents an analytical formulation based on the logarithmic law for the velocity profile of the compressible turbulent boundary. Integral parameters of the boundary layer such as the thickness, displacement thickness, and momentum thickness are determined. In due course, the author of Ref. 25 demonstrated that the analytical method yields somewhat better accuracy in comparison with the well-known empirical prediction procedure of Ref. 26. The method of the effective length of Ref. 27 was used to take into account the longitudinal gradients of the flow parameters at the external boundary of the viscous layer. With the use of these methods, a procedure for the boundary-layer calculation consists in the following. The calculation strip along a streamline on the surface is partitioned into a set of plane segments. The parameters of a local flow outside the boundary layer are taken from the known inviscid flowfield, and they are assumed to be constant within the segment. Calculation of the first segment is obvious. The boundary layer on each subsequent segment is calculated as on a flat plate with an effective length added upstream of the segment beginning. This length corresponds to the boundary-layer length determined by the local flow parameters using the conservation condition of the boundary-layer momentum thickness at the joint line of the foregoing and current segments. The effective length method holds the overall friction force of a calculated surface.

The viscous flow characteristics correspond to the flight regime with a dynamic pressure $q_\infty = 7 \times 10^4$ Pa and surface temperature $T_w = 800$ K. To determine the characteristic linear scale of waveriders, which is essential for the estimation of viscous effects, we set $R_0 = 10$ m, which corresponds to waverider lengths $L_w = 1.5$–3 m. The base pressure over the end cross section area was assumed to be equal to the freestream pressure, that is, the base drag was canceled.

The lift coefficient C_L for the considered waveriders is shown in Fig. 5 as a function of the relative radius $\bar{R}_e$ for several values of the

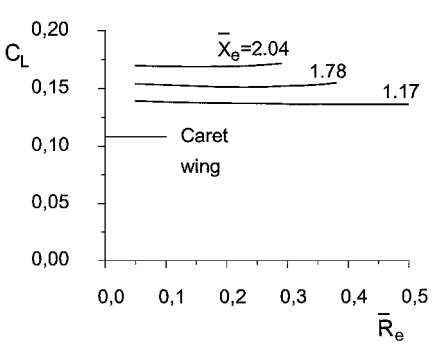

Fig. 5 Lift coefficient of convergent waveriders vs relative radius of transverse curvature of the lifting surface, $M_\infty = 6$: convergent waverider $\delta_d = 10$ deg and $\varphi = 45$ deg and caret wing $\delta_w = \delta_d = 10$ deg.

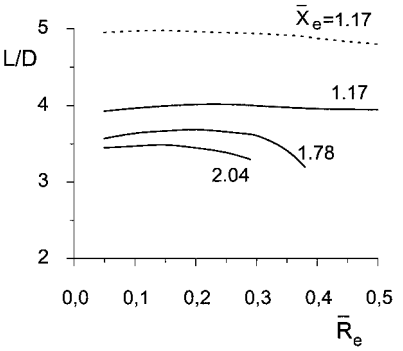

Fig. 6 Lift-to-drag ratio of convergent waveriders vs relative radius of transverse curvature of the lifting surface: $M_\infty = 6$, $\delta_d = 10$ deg, and $\varphi = 45$ deg.

coordinate $\bar{x}_e$. As the calculated data show, the magnitude of C_L is almost independent of $\bar{R}_e$ for the given value $\bar{x}_e = \text{const}$. Figure 5 shows the value of C_L for a simple Nonweiler caret wing,[6,7] which is equal to the pressure coefficient behind an oblique shock wave on a wedge with the angle $\delta_w = \delta_d$. This value, in fact, determines the lowest possible value of C_L of the waveriders examined when they are located at the upstream region of the basic flow in a constricting duct for $\bar{x}_e \to 0$. As should be expected from the basic flow features with a longitudinal pressure gradient, an increase in the parameter $\bar{x}_e$, that is, a more downstream displacement of the configurations constructed, leads to a significant growth of the lift coefficient. For example, C_L of waveriders with $\bar{x}_e = 1.17$, 1.78, and 2.04 are, respectively, 1.2, 1.4, and 1.6 times greater than that for the Nonweiler caret wing.[6,7] Thus, for equal values of the Mach number M_∞ and initial angle of flow deflection δ_d, waveriders based on the flow in a constricting duct ensure a significant advantage in the lift coefficient as compared with waveriders constructed from the uniform flow behind a plane shock wave. A downstream shift of the aerodynamic center of the convergent waveriders is obvious as compared with the uniform-flow-derived waveriders. This is caused by the mentioned pressure gradient downstream along the streamlines of the basic convergent flow.

The lift-to-drag ratio of the waveriders is presented in Fig. 6 as a function $L/D = f(\bar{R}_e)$ for several values of $\bar{x}_e$; the dashed curve corresponds to the estimate for an inviscid flow, and the solid curves refer to the estimates including friction drag forces. As for the lift force, the parameter $\bar{x}_e$ (the waverider position in the basic flowfield) exerts a determining effect on the lift-to-drag ratio. An increase in $\bar{x}_e$ leads to a decrease in the lift-to-drag ratio due to the shift of the designed waverider downstream in the basic flowfield. This decrease is caused by two factors. One is the increase in the relative area of the midsection coincident with the end cross section, that is, the increase in the value S_m / S_{pl} of the waverider. The other is the increase in flow compression and, consequently, a gradual increase in the pressure coefficient along the lifting surface. This means that, in terms of L/D values, the best waveriders lie as close as possible to the leading edge of the flow-generating duct where the local flow tends to two dimensional. The presence of a weak maximum in the dependence of the lift-to-drag ratio on the radius $\bar{R}_e$ should also be noted. As $\bar{x}_e$ decreases, the optimal values of $\bar{R}_e$ become higher. This means that the optimal radius of the lifting surface in the end cross section decreases as the waverider designed shifts to the region of a more compressed basic flow. Note, the values L/D properly become smaller with the decrease in the optimal values of $\bar{R}_e$.

Figure 7 shows the heat flux characteristics of the convergent waveriders determined in accordance with the preceding assumptions. The relative integral input heat flux is plotted as a function $\bar{Q} = f(\bar{R}_e)$ for a number of relative coordinates $\bar{x}_e$. For a fixed value $\bar{x}_e = \text{const}$, the integral input heat flux has a maximum. The latter is caused by the change in the relative total wetted area of the waverider surfaces in accordance with the change in the relative length $\bar{L}_w$ of a configuration with a maximum dependent on $\bar{R}_e$ (see Fig. 2). This

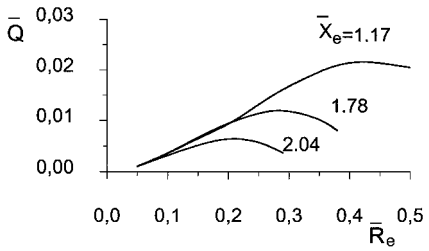

Fig. 7 Integral heat flux input to the convergent waverider body vs relative radius of transverse curvature of the lifting surface: $M_\infty = 6$, $\delta_d = 10$ deg, and $\varphi = 45$ deg.

is one of the major factors governing the level of the integral input heat flux for the waverider considered. As $\bar{x}_e$ increases, that is, as the configurations shift to the region of a more compressed flow, the heat transfer intensity increases. Nevertheless, the relative decrease in the wetted surface is again the factor determining a decrease in Q as a whole. Note that a sufficiently low level of the integral heat flux Q for $\bar{x}_e = \text{const}$ can be apparently achieved by means of a proper choice of $\bar{R}_e$ without significant losses in the lift coefficient and the lift-to-drag ratio.

The exemplified aerodynamic characteristics correspond to the half-angle of the arc sector of the lower surface in the end cross section $\varphi = 45$ deg. The calculations show that the drag C_D and the lift C_L coefficients slightly decrease with increasing φ, and the function of the lift-to-drag ratio $L/D = f(\varphi)$ has a weak maximum. At the same time, the change in aerodynamic characteristics is rather small within a wide range of practical interest, $30 < \varphi < 90$ deg.

In summary, the parametric analysis of the effect of independent parameters determining the geometry of the waveriders on their integral aerodynamic characteristics shows that the main factor is the position of the configuration considered in the basic flowfield, that is, the longitudinal coordinate $\bar{x}_e$ of the end cross section. The effect of the transverse curvature of the lifting surface characterized by its relative radius $\bar{R}_e$ and half-angle of the arc sector φ in the end cross section is small. At the same time, all of these independent parameters are essential from the viewpoint of their effect on the integral input heat flux.

Comparison of Various Types of Waveriders

Some characteristics of a convergent waverider and a simple waverider of a caret-wing type have been compared. For a more comprehensive estimate of the characteristics of the convergent waveriders, the two were also compared with a waverider of a common type designed with the use of an axisymmetric flow around a circular cone at zero incidence (Fig. 8). This flow is described by known ordinary differential equations, whose numerical solution presents no difficulties. In this case, the streamlines of the basic conic flow are diverging from the flow axis. Because of this, the streamlines of the flow under a cone-derived waverider constructed and the streamlines on the surface of its compression surface are also divergent. The procedure of designing the cone-derived waveriders and the limitations used are similar to those already described. In particular, the transverse-concave contour of the lifting surface in the end cross section was also prescribed by the arc of radius R_e. Note that waveriders with the transverse-concave trailing edge of a segment-circle shape, along with other different cross-sectional contours, are considered in the optimization of cone-derived waveriders.[28]

A typical feature of cone-derived waveriders is that their aerodynamic characteristics determined for an inviscid flow are independent of the longitudinal coordinate x_e because of flow conicity. This distinguishes them from the considered convergent waveriders whose longitudinal position in the basic flowfield is a factor that determines their aerodynamic characteristics. Consequently, the relative radius determining the transverse concavity of these waveriders was normalized by the length x_e, that is, in this case $\bar{R}_e = R_e/x_e$.

The aerodynamic characteristics of the convergent-flow-derived, cone-derived, and caret-wing-type waveriders are compared in Figs. 9 and 10 for the parameters $M_\infty = 6$, $\delta_d = 10$ deg, $\varphi = 45$ deg,

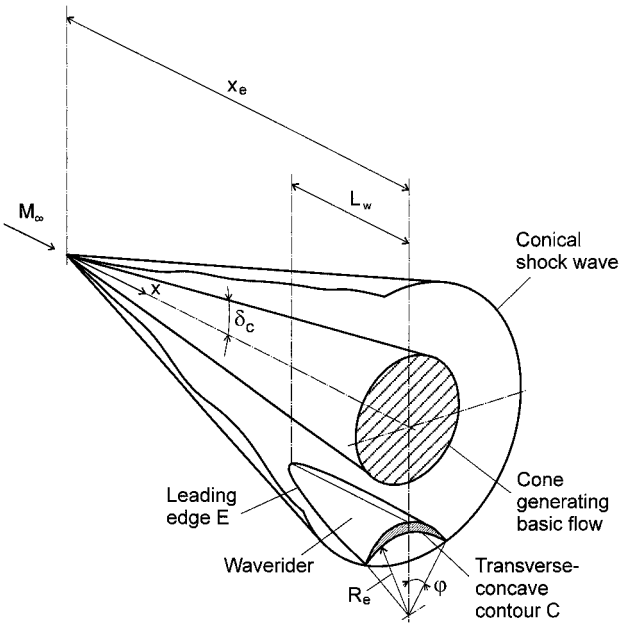

Fig. 8 Designing waveriders on the basis of the axisymmetric flow around a circular cone.

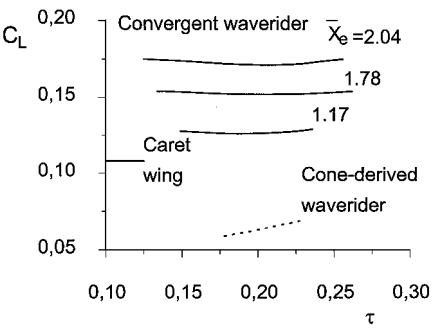

Fig. 9 Comparison of the lifting properties of different waveriders, $M_\infty = 6$: convergent waverider $\delta_d = 10$ deg and $\varphi = 45$ deg, cone-derived waverider $\delta_c = \delta_d = 10$ deg and $\varphi = 45$ deg, and caret wing $\delta_w = \delta_d = 10$ deg.

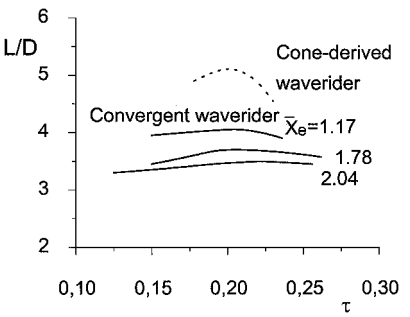

Fig. 10 Comparison of the lift-to-drag ratio of convergent and cone-derived waveriders, $M_\infty = 6$: convergent waverider $\delta_d = 10$ deg and $\varphi = 45$ deg and cone-derived waverider $\delta_c = \delta_d = 10$ deg and $\varphi = 45$ deg.

and $\delta_w = \delta_c = \delta_d$ as functions of the volumetric factor τ. The data show that, for a given value of τ, convergent waveriders exhibit significantly better lifting properties (see Fig. 9) as compared with cone-derived or caret waveriders. For the latter, the value of the lift coefficient C_L is determined only by the values of M_∞ and δ_w and does not depend on the volumetric factor τ. The increase in C_L with increasing τ for the cone-derived waverider is related to the shift of the lifting surface from the shock wave to the cone surface itself, that is, to the region of a more compressed basic flow. The last calculated point on the curves C_L vs τ for this waverider corresponds

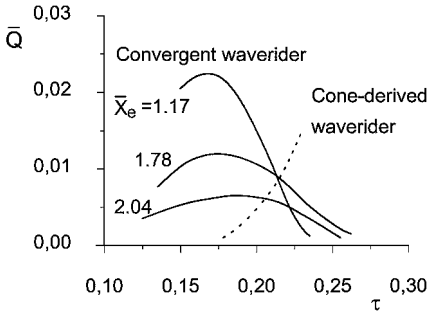

Fig. 11 Integral heat flux input through the surfaces of convergent and cone-derived waveriders, $M_\infty = 6$: convergent waverider $\delta_d = 10$ deg and $\varphi = 45$ deg and cone-derived waverider $\delta_c = \delta_d = 10$ deg and $\varphi = 45$ deg.

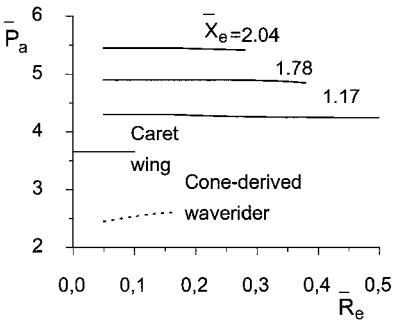

Fig. 12 Average static pressure in the airstream restricted by the shock wave and transverse contour of the lower lifting surface in the end cross section of different waveriders, $M_\infty = 6$: convergent waverider $\delta_d = 10$ deg and $\varphi = 45$ deg, cone-derived waverider $\delta_c = \delta_d = 10$ deg and $\varphi = 45$ deg, and caret wing $\delta_w = \delta_d = 10$ deg.

to the tangent point of the lifting surface and the surface of the flow-generating cone in the plane of symmetry. As shown in Ref. 29, this point is a local minimum of the lift-to-drag ratio. Despite high lifting properties, convergent waveriders have a lower lift-to-drag ratio as compared with cone-derived waveriders (see Fig. 10). This is related to a greater angle of inclination of the lifting surface to the freestream flow and to a greater level of flow compression along this surface for the convergent waverider. Note also that, for $R_e / L_w > 0.5$, the coordinate of the aerodynamic center of the convergent-flow-derived waveriders varies within $\bar{x}_a = 0.62$–0.68, depending on R_e / R_0 in the range of their considered values, whereas for the cone-derived waveriders it comprises $\bar{x}_a \approx 0.6$. That is, the aerodynamic center of the convergent-flow-derived waveriders shifts to the end cross section as compared with the conic-flow-derived waveriders. This shift is caused by the pressure gradient downstream along the streamlines of the basic flow.

The estimates of the integral input heat flux for the waveriders of different types considered are shown in Fig. 11. An increase in the volumetric factor τ for convergent waveriders is accompanied by a decrease in the lifting surface radius $\bar{R}_e$ in the end cross section and, hence, by the corresponding change in the waverider length $\bar{L}_w$ (see Fig. 2). Thus, those values of τ that ensure the maximum length of the waverider correspond also to the maximum of $\bar{Q}$. For cone-derived waveriders, the increase in τ is related to the increase in the radius $\bar{R}_e$ and the length $\bar{L}_w$, which leads to a monotonic increase in $\bar{Q}$. Therefore, for high values of τ, cone-derived waveriders can also have a higher level of the integral input heat flux. Thus, apart from a higher lift coefficient, convergent waveriders can also ensure lower levels of the integral heat flux for high values of the volumetric factor τ.

For a comparative estimate of the characteristics of convergent waveriders as forebodies with a transverse-concave lifting–compressing surface, we determined the average parameters of an airstream captured by an inlet arranged downstream from the waverider end cross section. The lifting surface of the waverider and the shock wave bound this stream here. For the said stream, in particular, we determined the parameter A_∞ / S_{pl}, where A_∞ is the cross-sectional area of the free airstream that could be captured by an inlet. This parameter is equivalent to the inlet mass-flow-rate factor and characterizes the ability of the lifting configuration to serve as an inlet precompression body, that is, to capture the airstream by its leading edges. For the waveriders under consideration, we have $A_\infty / S_{\text{pl}} = 0.34$–$0.42$, ~ 0.32, and ~ 0.25 for the convergent, caret, and cone-derived waveriders, respectively. Thus, the convergent waverider has a certain advantage in this characteristic.

The average parameters of the inlet-captured airstream in the end cross section, that is, the Mach number M_a, the relative static pressure $\bar{p}_a = p_a / p_\infty$, etc., were determined from the conditions of conservation of the flow rate, total energy, and entropy, following Ref. 30. It was assumed that the equivalent averaged flow is to be directed along the lifting surface of the waverider. This averaging is used for its equivalence to conservation of the engine stream workability, which is essential under consideration of fuel-economic performance of an airbreathing engine. Note, in contrast to this, the stream entropy is not conserved at averaging with conservation of the flow momentum. Note also that, for high flow Mach number $M > 1.3$–1.5, both schemes of averaging with conservation of either the momentum or the entropy give parameters of equivalent averaged one-dimensional streams differing by only fractions of a percent.[30] Figure 12 shows an example of the relative average pressure $\bar{p}_a$ vs the relative waverider radius $\bar{R}_e$ in the end cross section for some values of $\bar{x}_e$. The characteristics of all of the waveriders discussed are presented. The average pressure of the inlet-captured airstream is almost independent of $\bar{R}_e$ for the convergent and cone-derived waveriders, and it is constant for the caret waverider. The compression level of the said airstream for the convergent waveriders increases as the coordinate $\bar{x}_e$ increases, and it is significantly higher than that for the equivalent Nonweiler caret wing[6,7] and the cone-derived waverider.

Conclusions

A class of convergent waveriders designed on the basis of supersonic axisymmetric compression flows inside constricting ducts has been considered. The streamlines of the basic flows are convergent to the flow axis, and the flow near the lifting surface of the waveriders is also convergent. Simple convergent waveriders with a lifting surface of transverse-concave arc-shaped contour were designed using the flow inside conical ducts–trumpets. It is shown that the main factor that determines the level of the aerodynamic characteristics of the waveriders is the longitudinal position of a constructed configuration in the basic flowfield. By varying this position while designing the waverider, it is possible to achieve some compromise between the possible high lift coefficient and the reachable lift-to-drag ratio.

The level of the integral input heat flux to the convergent waverider body substantially depends on the curvature radius of the transverse contour of the lifting surface in the end cross section. It can be decreased by choosing a proper value of this radius, which has an insignificant effect on the lifting properties and the lift-to-drag ratio of the waveriders. Convergent waveriders can ensure low levels of the integral heat flux at high values of the volumetric factor of the lifting configuration.

The class of waveriders under study can exhibit significantly higher values of the lift coefficient in comparison with equivalent waveriders derived from flows around a wedge or a circular cone. In this aspect, the convergent waveriders can be of interest for solving the problems of reentry hypersonic flying vehicles, when configurations producing a large lift force are needed to ensure maneuverability of the vehicle.

In addition, convergent waveriders have also an elevated level of flow compression near the lower lifting surface. Thus, they can be used for airbreathing-engine-powered hypersonic vehicles as forebodies with a flow precompression surface upstream of the inlet. Arrangement of convergent waveriders with convergent inlets also designed from internal supersonic compression flows using the same principles is of particular interest in this aspect.

References

[1]Küchemann, D., "Hypersonic Aircraft and Their Aerodynamic Problems," *Progress in Aeronautical Sciences*, Vol. 6, edited by D. Küchemann and L. H. G. Stern, Pergamon, Oxford, England, U.K., 1965, pp. 271–353.

[2]Küchemann, D., *The Aerodynamic Design of Aircraft*, Pergamon Press, London, 1978, Chap. 8.

[3]Jones, J. G., Moore, K. C., Pike, J., and Roe, P. L., "A Method for Designing Lifting Configurations for High Supersonic Speeds, Using Axisymmetric Flow Fields," *Ingenieur Archiv*, Vol. 37, No. 1, 1968, pp. 56–72.

[4]Seddon, J., and Spence, A., "The Use of Known Flow Fields as an Approach to the Design of High Speed Aircraft," CP-30, AGARD, 1968, pp. 10/1–10/21.

[5]Maikapar, G. I., and Keldysh, V. V., "Gasdynamic Design of Hypersonic Aircraft," *Izvestiya AN SSSR, Mechanica Zhidkosti i Gaza (Fluid Dynamics)*, No. 3, 1969, pp. 177–185 (in Russian).

[6]Nonweiler, T., "Aerodynamic Problems of Manned Space Vehicles," *Journal of the Royal Aeronautical Society*, Vol. 63, No. 589, 1959, pp. 521–528.

[7]Nonweiler, T., "Delta Wings of Shapes Amenable to Exact Shock Wave Theory," *Journal of the Royal Aeronautical Society*, Vol. 67, No. 625, 1963, pp. 39, 40.

[8]Maikapar, G. I., "Bodies Formed by the Stream Surfaces of Conical Flows," *Izvestiya AN SSSR, Mechanica Zhidkosti i Gaza (Fluid Dynamics)*, No. 1, 1966, pp. 126, 127 (in Russian).

[9]Rasmussen, M. L., "Waverider Configurations Derived from Inclined Circular and Elliptic Cones," *Journal of Spacecraft and Rockets*, Vol. 17, No. 6, 1980, pp. 537–545.

[10]Rasmussen, M. L., and Clement, L. W., "Cone-Derived Waveriders with Longitudinal Curvature," *Journal of Spacecraft and Rockets*, Vol. 23, No. 5, 1986, pp. 461–469; also AIAA Paper 84-2100, Aug. 1984.

[11]Townend, L. H., "On Lifting Bodies of Delta Planform Which Can Support Plane Attached Shock Waves," A.R.C. Repts. and Memoranda 3383, Her Majesty's Stationary Office, London, England, UK, 1963.

[12]O'Neil, M. K. L., and Lewis, M. J., "Optimized Scramjet Integration on a Waverider," *Journal of Aircraft*, Vol. 29, No. 6, 1992, pp. 1114–1121.

[13]Molvik, G., Bowles, J., and Huynh, L., "A Hypersonic Waverider Research Vehicle with Hydrocarbon Scramjet Propulsion: Design and Analysis," AIAA Paper 93-5097, Nov. 1993.

[14]Goonko, Y. P., "Gasdynamic Design of Aerodynamic Configurations with Convergent Compression Surfaces and Inlets," *Mathematical Modeling, Aerodynamics, and Physical Gasdynamics*, edited by V. M. Fomin, Inst. of Theoretical and Applied Mechanic of Siberian Branch of Academy of Sciences of the Union of Soviet Socialist Republics, Novosibirsk, Russia, 1995, pp. 133–142 (in Russian).

[15]Goonko, Y. P., "Aerodynamic Configurations of Hypersonic Airbreathing Vehicles with Convergent Inlets," *Tehnika Vozdushnogo Flota (Airfleet Machinery–Journal of Aviation Science and Technology)*, No. 5–6, 1996, pp. 63–71 (in Russian).

[16]Blokhin, A. M., Gutov, B. I., Zatoloka, V. V., Vetlutskaya, L. M., Dolgov, V. N., and Shumsky, V. V., "Convergent Inlet Diffusers and Axisymmetric Supersonic Compression Busemann Flows," *Aerophysical Studies*, Inst. of Theoretical and Applied Mechanic of Siberian Branch of Academy of Sciences of the Union of Soviet Socialist Republics, Novosibirsk, Russia, No. 1, 1972, pp. 105–108 (in Russian).

[17]Gutov, B. I., and Zatoloka V. V., "Convergent Inlet Diffusers with the Initial Shock Wave and Additional External Compression," *Aerophysical Studies*, Inst. of Theoretical and Applied Mechanic of Siberian Branch of Academy of Sciences of the Union of Soviet Socialist Republics, Novosibirsk, Russia, No. 2, 1973, pp. 64–66 (in Russian).

[18]Shchepanovsky, V. A., and Gutov, B. I., *Gasdynamic Design of Supersonic Inlets*, Nauka, Novosibirsk, Russia, 1993 (in Russian).

[19]Goonko, Y. P., Markelov, G. N., and Shashkin, A. P., "Gasdynamic Design of Waveriders with Convergent Compression Surfaces and Inlets," *Sibirsky Phiziko-Tehnichesky Zhurnal (Siberian Physical–Technical Journal)*, No. 4, 1993, pp. 47–55 (in Russian).

[20]Ferri, A., "The Method of Characteristics," *High Speed Aerodynamics and Jet Propulsion: General Theory of High Speed Aerodynamics*, Princeton Series, edited by W. R. Sears, Vol. 6, 1954, Sec. G, Chap. 4.

[21]Ehlers, F. E., "The Method of Characteristics for Iso-Energetic Supersonic Flows Adapted to High-Speed Digital Computers," *Journal of Industrial and Applied Mathematics*, Vol. 7, No. 1, 1959.

[22]Katskova, O. N., and Chushkin, P. I., "Three-Dimensional Supersonic Equilibrium Flow of a Gas Around Bodies at Angle of Attack," NASA TTF-9790, Dec. 1965.

[23]Katskova, O. N., Naumova, I. N., Shmyglevsky, Y. D., and Shchulishina, N. P., *Experience of Calculation of Two-Dimensional and Axisymmetric Supersonic Gas Flows by the Method of Characteristics*, Computing Center, USSR Academy of Science, Moscow, 1961 (in Russian).

[24]Lee, B. H. K., "Numerical Calculations of Hypersonic Viscid–Inviscid Flows Inside Simple Ducts of Circular Cross Section," *Aeronautical Quarterly*, Vol. 22, Pt. 3, 1971, pp. 233–256.

[25]Kovalenko, V. M., "Calculation of Friction and Heat Transfer Coefficients of a Flat Plate at Supersonic Speeds in the Presence of Heat Exchange," *Trudy TsAGI (Proceedings of Central Aerogydrodynamic Institute–CAGI)*, CAGI, Moscow-Zhukovsky, No. 1084, 1967, pp. 1–51 (in Russian).

[26]Spalding, D. B., and Chi, S. W., "The Drag of a Compressible Turbulent Boundary Layer on a Smooth Flat Plate With and Without Heat Transfer," *Journal of Fluid Mechanics*, Vol. 18, Pt. 1, 1964, pp. 117–143.

[27]Repik, E. U., "Approximate Calculation of a Turbulent Boundary Layer in a Compressible Fluid with Pressure Gradients," *Technicheskie Otchety TsAGI (Technical Reports of the Central AeroGydrodynamic Institute–CAGI)*, No. 167, 1960, pp. 12–21 (in Russian).

[28]Kim, B. S., Rasmussen, M. L., and Jischke, M. C., "Optimization of Waverider Configurations Generated from Axisymmetric Conical Flows," *Journal of Spacecraft and Rockets*, Vol. 20, No. 5, 1983, pp. 461–469.

[29]Mazhul, I. I., "Aerodynamics of Lifting Waveriders Constructed on the Basis of Axisymmetric Conic Flows," *Thermophysics and Aeromechanics*, Vol. 3, No. 4, 1996, pp. 327–332.

[30]Cherkez, A. Y., "On Some Properties of Averaging the Supersonic Gas Flows," *Izvestiya AN SSSR, Otdelenie technichkih nauk (News of Academy of Sciences of USSR, Technical Sciences Branch)*, No. 4, 1962, pp. 22–26 (in Russian).